Research Article | Vol. 9, No. 11 | 1 Nov 2018 | BIOMEDICAL OPTICS EXPRESS 5583
Biomedical Optics EXPRESS

Automated instrument designed to determine visual photosensitivity thresholds

MARIELA C. AGUILAR,[1,2] ALEX GONZALEZ,[1] CORNELIS ROWAAN,[1] CAROLINA DE FREITAS,[1] KARAM A. ALAWA,[1] HEATHER DURKEE,[1,4] WILLIAM J. FEUER,[3] FABRICE MANNS,[1,4] SHIHAB S. ASFOUR,[2] BYRON L. LAM,[3] AND JEAN-MARIE A. PAREL[1,4,5,*]

[1]*Ophthalmic Biophysics Center, Bascom Palmer Eye Institute, Department of Ophthalmology, University of Miami Miller School of Medicine, Miami, FL, USA*
[2]*Department of Industrial Engineering, College of Engineering, University of Miami, Coral Gables, FL, USA*
[3]*Anne Bates Leach Eye Center, Bascom Palmer Eye Institute, Department of Ophthalmology, University of Miami Miller School of Medicine, Miami, FL, USA*
[4]*Department of Biomedical Engineering, College of Engineering, University of Miami, Coral Gables, FL, USA*
[5]*Brien Holden Vision Institute, University of New South Wales, Sydney, Australia*
**jmparel@med.miami.edu*

Abstract: The Ocular Photosensitivity Analyzer (OPA), a new automated instrument to quantify the visual photosensitivity thresholds (VPT) in healthy and light sensitive subjects, is described. The OPA generates light stimuli of varying intensities utilizing unequal ascending and descending steps to yield the VPT. The performance of the OPA was evaluated in healthy subjects, as well as light sensitive subjects with achromatopsia or traumatic brain injury (TBI). VPT in healthy, achromatopsia, and TBI subjects were 3.2 ± 0.6 log lux, 0.5 ± 0.5 log lux, and 0.4 ± 0.6 log lux, respectively. Light sensitive subjects manifested significantly lower VPT compared to healthy subjects. Longitudinal analysis revealed that the OPA reliably measured VPT in healthy subjects.

1. Introduction

Photophobia, first described as an abnormal intolerance to light [1], is a disorder that affects up to 25% of the population. Photophobia, also referred to as visual photosensitivity [2], is commonly associated with numerous ophthalmic and neurologic pathologies [3–5], such as dry eye [3,4,6,7], blepharospasm [3–5,8–10], migraine [3–5,11–18], traumatic brain injury (TBI) [4,5,8,19–25], and genetic disorders such as achromatopsia [3,4,26], retinitis pigmentosa [3,4], and other retinal dysfunctions [3,4]. Since visual photosensitivity is associated with various ophthalmic and neurologic pathologies, quantifying the visual photosensitivity thresholds (VPT) of these individuals may help determine the progression and severity of these disorders.

A few studies have been conducted to quantify visual photosensitivity. Wirtschafter and Bourassa [27–29] investigated the threshold of discomfort to bright light in normal subjects as well as subjects with neurologic and ophthalmic disorders. They positioned the subjects 50 cm from a large translucent screen marked at the center with a 6 cm fixation target. Four fluorescent lights and two incandescent spotlights aimed at the center of the screen were positioned behind the translucent screen. The luminance of the sources was modified using a motor operated transformer that directly regulated the voltage to the lamps. The subjects were instructed to look at the fixation target and to press a large red button located in front of them as soon as the light became uncomfortable. The luminance at which the subject pressed the button was considered to be the VPT for the trial. The illumination increased from its lowest

#341567 https://doi.org/10.1364/BOE.9.005583
Journal © 2018 Received 7 Aug 2018; revised 1 Oct 2018; accepted 2 Oct 2018; published 18 Oct 2018

Biomedical Optics EXPRESS

to its highest value in 15 seconds. The variability of the measured VPTs prevented reliable group comparisons.

Vanagaite et al. [12] measured light discomfort thresholds in individuals with migraine, cervicogenic headache [30], cluster headache [31] and compared to control subjects. They used a high power (800 - 1000 W) halogen lamp connected to a rheostat, a modified slit-lamp chin and forehead rest, and heat filters, which blocked a portion of the infrared radiation. Illuminance was measured with a photometer and the subject reported to the operator verbally when the illuminance became uncomfortable. Adams et al. [8] used a similar system and methodology to measure light sensitivity of subjects with benign essential blepharospasm, migraine and compared to control subjects. Cortez et al. [32] further modified the system from Adams et al. [8] to include recording and offline processing of pupil responses during photophobia threshold testing in migraine and non-migraine subjects. In these previous studies, non-control subjects were found to be more light sensitive than control subjects. However, these systems had limitations. They were bulky laboratory instruments requiring significant operator verbal instruction input, generated a significant amount of heat, and were subject to spectral as well as power fluctuation of thermal light sources.

These few previous studies on photosensitivity relied on rudimentary laboratory setups that are not suitable for use in the clinic, are difficult to reproduce in a consistent manner, and are therefore not appropriate for comparative, multicenter, or quantitative studies. There is currently no clinically available instrument or standard protocol to quantitatively assess visual photosensitivity. The lack of reliable, standardized testing protocols and assessment tools for evaluating visual photosensitivity have led to different definitions and criteria of what it means to be “photosensitive”. A quantifiable standardized measure would allow us to better understand visual photosensitivity as it relates to different diseases and disorders.

Our goal is to design a novel compact automated computer-controlled instrument to reliably quantify VPT to facilitate assessment of disease severity and enable monitoring of both disease progression and efficacy of treatments over time. In this manuscript, the design, construction, and testing of the Ocular Photosensitivity Analyzer (OPA) and VPT measurements of both healthy and light sensitive subjects with achromatopsia or traumatic brain injury are presented.

2. Ocular Photosensitivity Analyzer

2.1 Design of OPA

The OPA consists of a computer-controlled LED array mounted on a stand with an adjustable head-chin rest, a video camera that records infrared images of the subject's face, a push button, and a laptop computer (Fig. 1). The light source consists of 210 white light emitting diodes (LED) (COM-11118, White – 10 mm, Sparkfun, Niwot, CO). The LEDs are assembled in a custom-built three-dimensional printed polymer-resin bi-cupola curved surface (BIONIKO Consulting, LLC, Miami, FL) mounted on an enclosure (WA-35, Polycase, Avon, OH). The left and right halves of the array each form a curved surface with its center of curvature located at the position of the left eye and right eye, respectively. The distance between the array and subject's eyes is 50 cm. At that distance, the entire LED array covers a field of view (angular subtense of the 23 cm wide array as seen by the subject) of 26 degrees. The LED array is viewed directly by the subject, no diffuser is used. Therefore, the retinal image is a grid of 210 individual LED images.

An additional single blinking white LED producing an illuminance of 0.14 lux (RL5-BW1520, Cool White – 5 mm, Super Bright LEDs Inc., St. Louis, MO) is located in the center of the bi-cupola for visual fixation. The blink frequency is 2 Hz. A miniature near-infrared camera (UI-5241LE, Imaging Development Systems Inc., Woburn, MA) for subject imaging and recording is integrated in the LED array enclosure with a single 850 nm infrared LED (HIR8323/C16, Everlight Americas Inc., Carrollton, TX) for illumination and a 850 nm

Biomedical Optics EXPRESS

near-IR bandpass filter (BP850, Midwest Optical Systems Palatine, IL). The camera records the subject's eyes at 60 frames/second.

The LED array, video camera, and handheld push-button (Delcom Engineering, Rye Brook, NY) are controlled using a touch screen laptop computer (Lenovo ThinkPad Twist S230u, Lenovo, Morrisville, NC) operating a customized control application developed with LabVIEW System Design Software (National Instruments, Austin, TX). The laptop computer, light source, and head-chin rest are mounted on a height-adjustable motorized electric table (ET175, Luxvision, US Ophthalmic, Doral, FL). Ambient temperature, humidity and light levels in the examination room are continuously measured with a temperature and humidity detector (AcuRite 00613A1, Acu-Rite Co Inc. Jamestown, NY) and a lux meter (Dr. Meter LX1010B, Hisgadget Inc., Union City, CA).

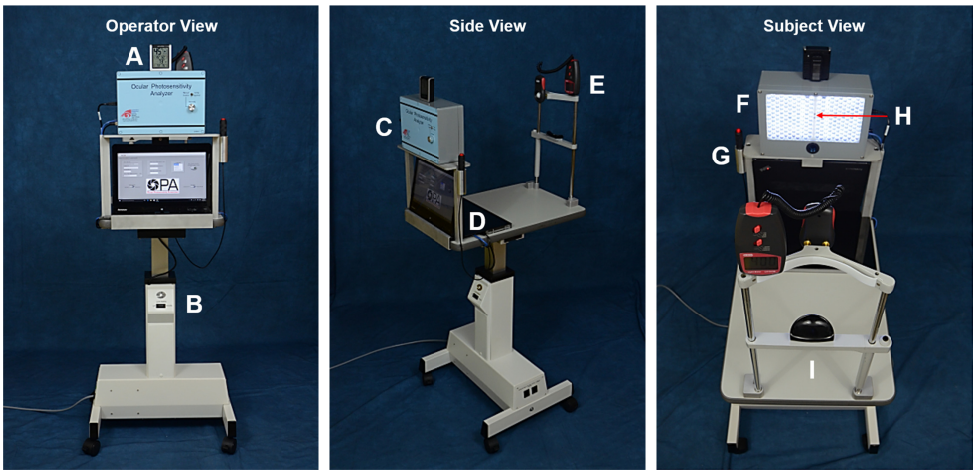

Fig. 1. The Ocular Photosensitivity Analyzer viewed from three perspectives. Operator View: A. Humidity and temperature meter, B. Table height adjustment controller; Side View: C. LED light source, D. Computer and graphical user interface, E. Lux meter; Subject View: F. LED concave array panel and integrated near infrared video camera, G. Handheld push-button, H. Single blinking white LED for fixation, I. Head-chin rest.

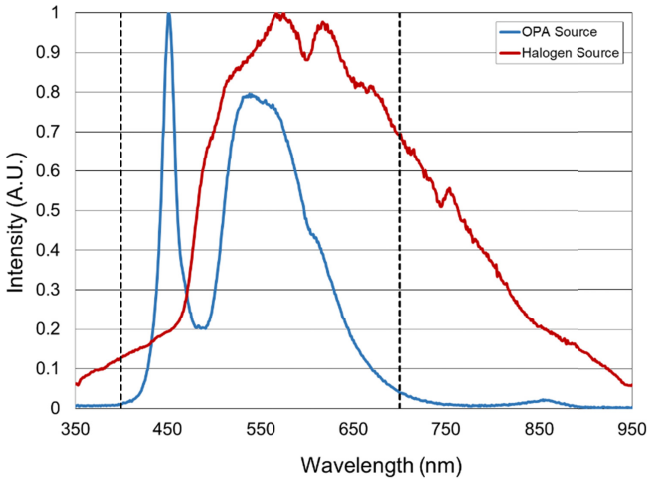

Fig. 2. Normalized emission spectrum of the OPA and Halogen source (Ianebeam halogen lamp with heat filter controlled by a rheostat as used by Vanagaite et al. [12] and Adams et al. [8]) from 350 to 950 nm. The visible spectrum range (400 to 700 nm) [33] is indicated by the two vertical black dashed lines.

Biomedical Optics EXPRESS

Based on preliminary testing, the OPA was designed to produce light stimuli ranging from 1 to 32,000 lux (0 to 4.5 log lux) measured at the positions of the subject's left and right eyes. The levels of the light stimuli were measured in lux and transformed logarithmically (log lux), as brightness of light sensation and intensity of the light stimulus have a logarithmic relationship [8,12,31,34]. For initial calibration, and light safety analysis the OPA LED array output was adjusted using a calibrated light meter (X1, Gigahertz-Optik, Inc., Newburyport, MA). The spectral output of the OPA LED array was measured with a spectrometer (SM442, Spectral Products, Putnam, CT) (Fig. 2). The device's light output was found to produce a retinal irradiance of 0.3 W/cm^2 at maximum intensity, well below the exposure limits set forth by the International Organization for Standardization (ISO) standard for ophthalmic instruments (ISO 15004-2, 2007).

2.2 OPA pupil diameter, palpebral fissure height, and inter-blink interval

The Ocular Photosensitivity Analyzer can simultaneously quantify an individual's VPT as well as capture real-time infrared digital video of the subject throughout the measurement session. The digital video is post-processed using a custom LabVIEW software interface that outputs the following physiological parameters: pupil diameter, palpebral fissure height, and inter-blink interval. These physiological parameters are measured as a function of illuminance to provide additional insight into the factors associated with visual photosensitivity.

The custom LabVIEW software identifies the location of the pupil using the reflection of the infrared LED on the cornea. A region of interest created around this reflection is processed to extract the pupil contour, the upper and lower eyelid contours, and the palpebral fissure height. The pupil contour is fit to an ellipse and pupil diameter is calculated by averaging the major and minor axes of the ellipse. Blinks are detected through a combination of pattern matching and finding frames where the corneal reflection is not present. An inter-blink interval (IBI) is calculated by measuring the time elapsed between consecutive blinks. The pupil diameter, palpebral fissure height, and IBI are plotted with respect to illuminance during each frame (Fig. 3).

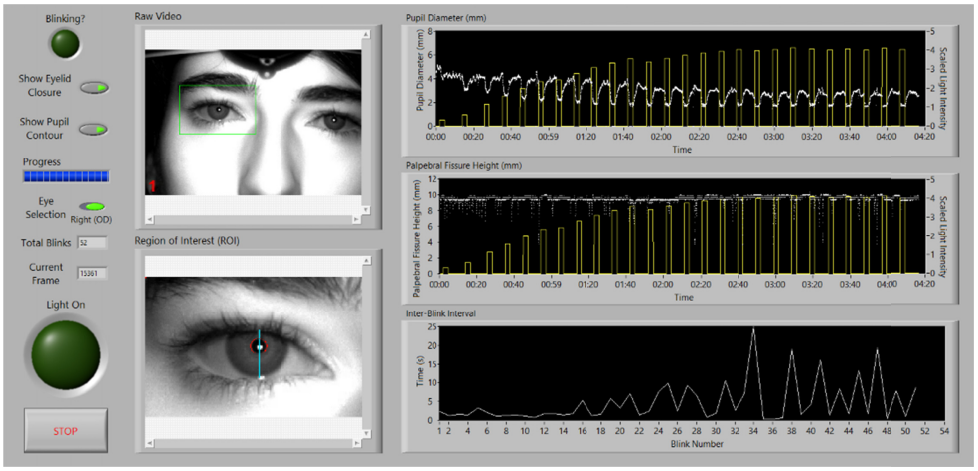

Fig. 3. Custom software interface used to post-process infrared video recordings. The software outputs the following physiologic parameters: pupil diameter, palpebral fissure height, and inter-blink interval (see Visualization 1).

3. Methods

3.1 Testing protocol

To minimize the effects of confounding variables during test administration, the testing protocol has been standardized by incorporating synthesized speech to administer test

Biomedical Optics EXPRESS

instructions and questions, in four languages (English, Spanish, French and Portuguese). The primary guideline is for the subject to indicate after each stimulus whether the light stimulus is uncomfortable by pressing a handheld push-button.

3.2 Testing paradigm

The automated instrument starts with the dimmest light stimulus and the stimulus intensity is gradually increased utilizing the Garcia-Perez staircase technique [35–37], which uses unequal ascending and descending steps. The total light stimuli range is divided into 100 steps (enhanced testing mode) or 25 steps (normal testing mode) depending on the severity of the subject's visual photosensitivity determined based on clinical symptoms.

Light stimuli are presented for a fixed duration of two seconds with a four second inter-stimulus rest period. During testing, the subject is queried if the previous stimulus was uncomfortable. They respond either yes (positive) with a button press or no (negative) with no button press. A subject's discomfort response based on their button press, will either increase or decrease the brightness for the next stimulus.

A response reversal is defined as when a subject's current response is different from the previous stimulus response, changing from yes (positive) to no (negative) or vice versa. The test concludes after 10 response reversals and the visual photosensitivity threshold is calculated from the mean of the illuminance recorded at the 10 response reversals (Fig. 4).

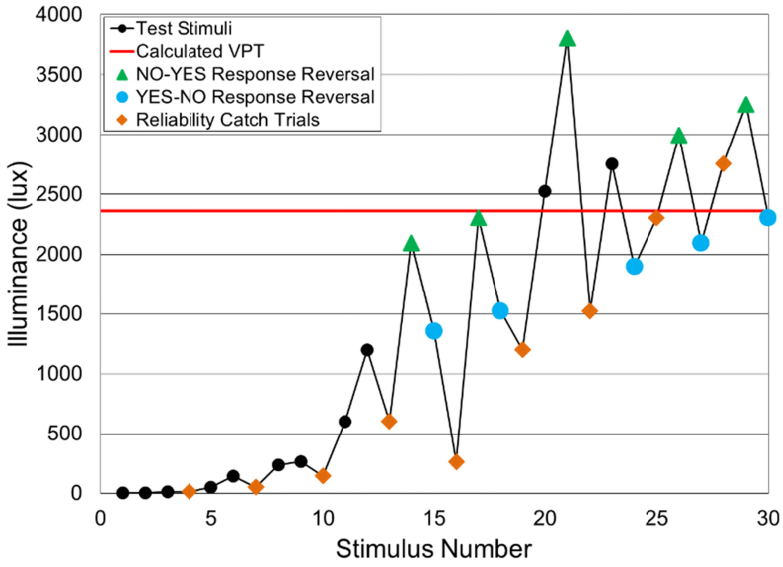

Fig. 4. Example of a response curve. The software automatically assesses the subject's visual photosensitivity threshold from the mean of 10 response reversals (For clarity, the green triangles and blue points have been added to delineate between response reversals and the orange diamonds represent catch trials).

Additionally, the device integrates a subject response reliability measure by utilizing catch trials throughout the testing paradigm. With the exception of the first stimulus, every third stimulus is a catch trial. In our system a catch trial is defined as a repetition of a randomly-selected previous stimulus. The subject's response to the previously administered stimulus is compared to that of the catch trial stimulus for consistency, from which a positive/negative inconsistency index score is computed (Fig. 5).

Biomedical Optics EXPRESS

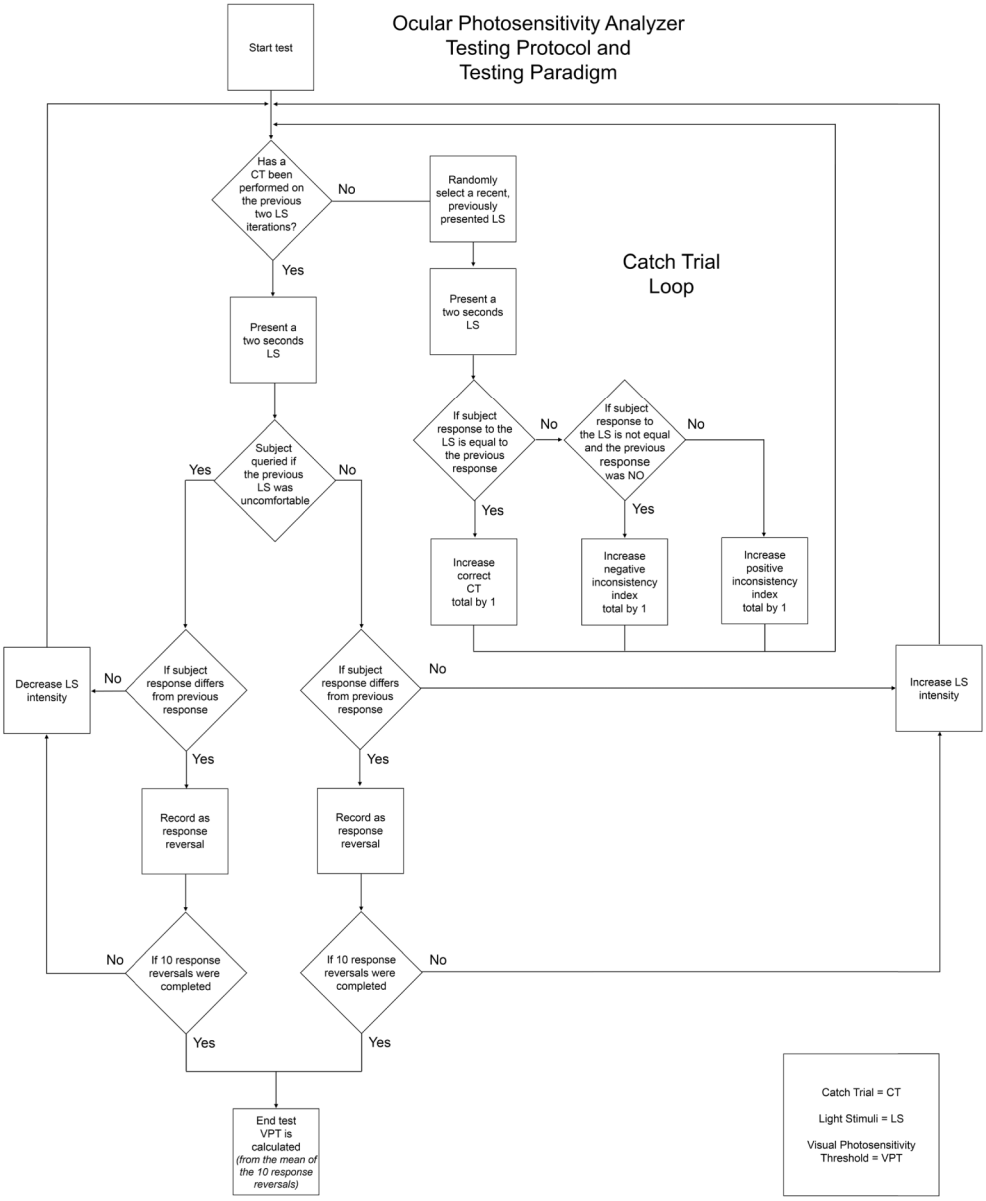

Fig. 5. Ocular Photosensitivity Analyzer Testing protocol and testing paradigm flowchart.

3.3 Subject testing protocol

The study was approved by the University of Miami Institutional Review Board. Informed consent was obtained from all subjects. Exam room lighting was adjusted to 4 lux (Mesopic illumination [38]) prior to subject arrival and a five minute adaptation period at minimum was implemented for all subjects. Spectacles and contact lenses were removed prior to testing to avoid optical interference due to tint, anti-reflective coatings, etc. Both eyes were tested simultaneously without pupil dilatation or ophthalmic medication.

In an effort to mitigate confounding variables, healthy subjects were measured at each time point at the same time of day as well as were queried about any unusual circumstances such as sleep hygiene, caffeine intake, mood, and prescription medications that may attribute

Biomedical Optics EXPRESS

to testing variability. Subjects were positioned properly on the head-chin rest and the height of the table and head-chin rest was adjusted to center the subject's eyes on the monitor's green line corresponding to the center of the LED array (Fig. 6). The subject was instructed to focus and maintain fixation at all times on the single blinking white LED at the cupola center. Once the subject was correctly positioned and ready, the operator started the automated testing session.

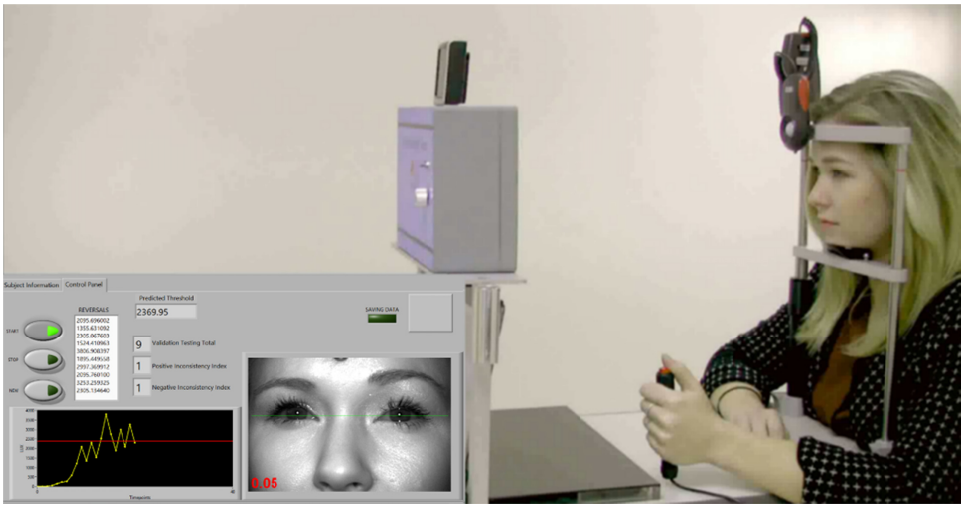

Fig. 6. The OPA testing a healthy subject and graphical user interface displaying subject's visual photosensitivity threshold in real-time.

4. Results

4.1 Longitudinal and reproducibility analysis of visual photosensitivity thresholds

Nine healthy subjects (five females and four males, age = 31.4 ± 7.6 y/o, range: 25 to 46 y/o) were tested. The refractive state was not assessed as part of these studies. The VPT of these subjects was measured at 0, 2, 12, 40, and 379 days (Fig. 7 and Fig. 8). Repeat VPT measurements (five time points) collected on healthy subjects over one year have shown excellent reproducibility (Intraclass Correlation Coefficient = 0.82) [39]. The VPT between 0 and 379 days amongst the healthy subjects ranged from 1.6 – 4.1 log lux; the overall mean across all sessions and subjects was 3.3 ± 0.5 log lux (Fig. 8). On average, no significant change was noted for the healthy subjects (Fig. 8, $p = 0.98$), demonstrating the reliability of the OPA.

Biomedical Optics EXPRESS

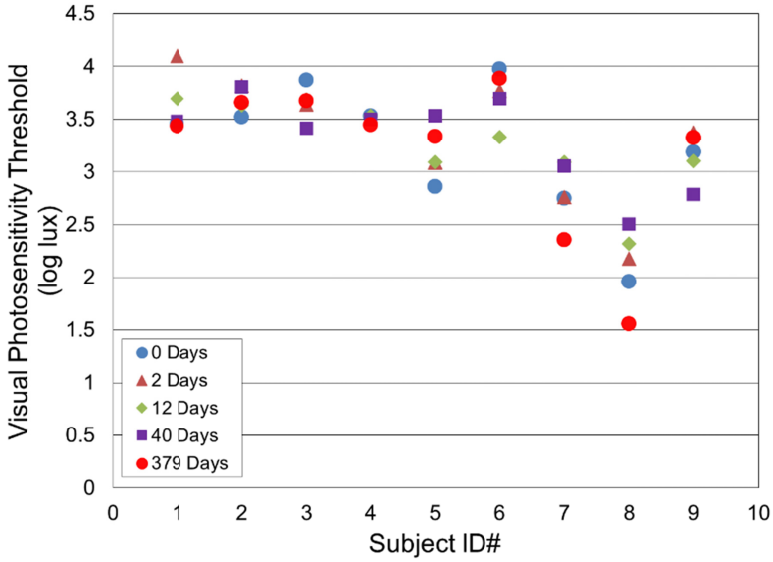

Fig. 7. Longitudinal visual photosensitivity thresholds assessment of healthy subjects at varying time points.

The VPT of one of the healthy subjects (ID#8) was significantly lower than average, for unknown reasons. The subject was emmetropic and reported having no visual/ocular abnormalities. A larger subject population is needed to determine more precisely where this subject fits in the distribution of VPT for healthy subjects.

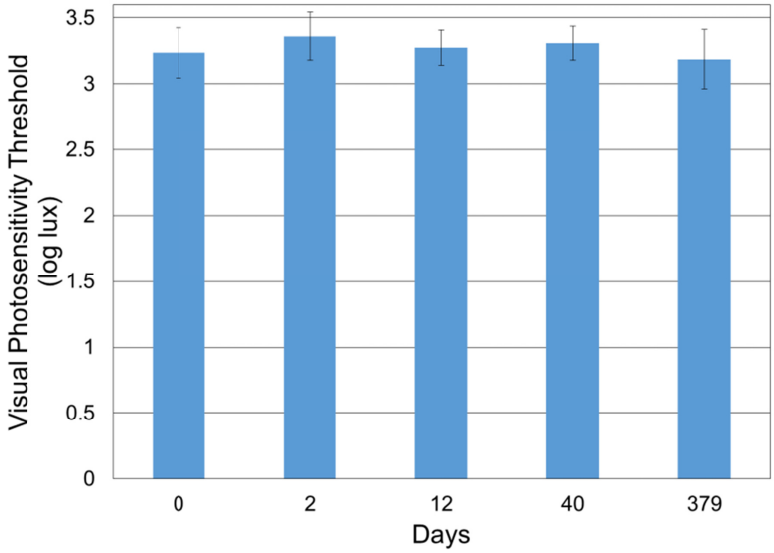

Fig. 8. The mean visual photosensitivity threshold (log lux) per time point: 0, 2, 12, 40, and 379 days (± Standard Error) of healthy subjects.

4.2 Visual photosensitivity thresholds of healthy, achromatopsia, and traumatic brain injury subjects

The VPT of the same nine healthy subjects from the longitudinal analysis was compared to the VPT of subjects with either achromatopsia, or TBI. Nine subjects with genetically verified

Biomedical Optics EXPRESS

CNGB3 or CNGA3 achromatopsia (six females and three males, age = 17.2 ± 7.9 y/o, range: 6 - 31 y/o) and three TBI subjects with dry eye symptoms (three males, age = 64.0 ± 19.1 y/o, range: 44 to 82 y/o) were tested. The mean measured VPT in healthy, achromatopsia, and TBI subjects were 3.2 ± 0.6 log lux, 0.5 ± 0.5 log lux, and 0.4 ± 0.6 log lux, respectively (Fig. 9).

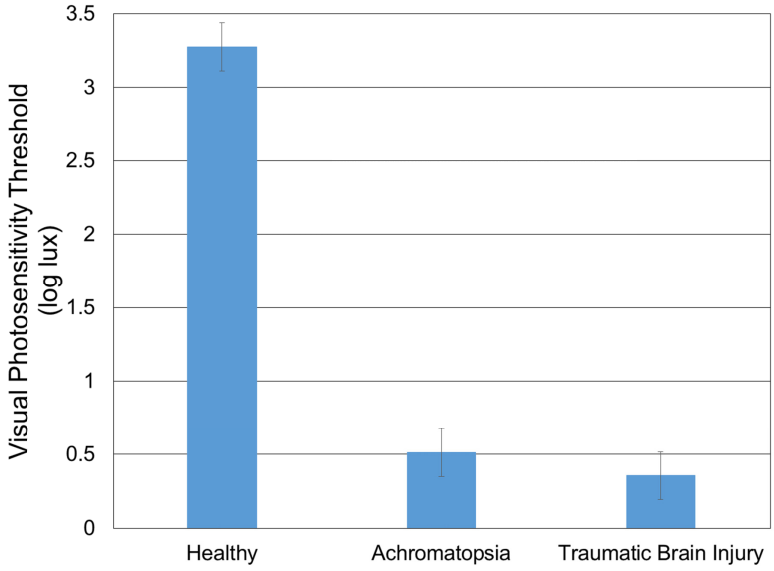

Fig. 9. Visual photosensitivity thresholds of healthy, achromatopsia, and TBI subjects (± Standard Error).

One-way analysis of variance showed a statistically significant difference ($p<0.0001$) in the visual photosensitivity threshold with higher thresholds in healthy subjects compared to light sensitive (achromatopsia and TBI) subjects. Overall catch trial accuracy (response inconsistency) for healthy subjects was 79.3% ± 13.4 with positive response inconsistencies accounting for 19.9% ± 14.6 and negative response inconsistencies 1.7% ± 3.7.

4.3 Pupil diameter and palpebral fissure height assessment

Videos from six healthy subjects (three females and three males, age = 30.2 ± 8.8 y/o, range: 23 to 45 y/o) were post-processed using the customized LabVIEW Software. The videos were calibrated from pixels to millimeters by imaging a machinist precision stainless steel ruler attached to the forehead rest. The calibration factor was 6 pixels/mm. As the distance between the subject's head and the camera is approximately the same for all subjects (50 cm), the same calibration factor was used for all experiments. In order to assess the accuracy of the software in measuring pupil diameter and palpebral fissure height, 10 frames from each video were randomly selected and analyzed manually using MATLAB. These measurements were then compared with those outputted by the software (Fig. 3).

A Bland-Altman analysis was performed on pupil diameter and palpebral fissure distance comparing automatic segmentation and manual segmentation methods [40,41]. The Bland-Altman scatterplots showed agreement between the automated segmentation method and manual segmentation method for both pupil diameter (Fig. 10) and palpebral fissure height (Fig. 11). The mean difference (± 2 SD) between manual and automated pupil diameter measurements was - 0.2 ± 0.4 mm. The mean difference (± 2 SD) for the palpebral fissure height measurements was 0.2 ± 1.0 mm. The larger variability of the palpebral fissure height measurements is due to a larger variability in the segmentation of the eyelid boundary.

Biomedical Optics EXPRESS

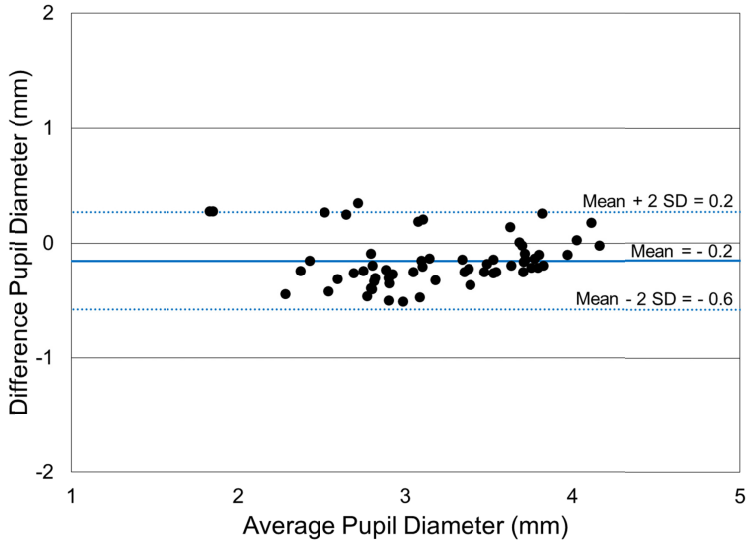

Fig. 10. Bland-Altman scatterplot of pupil diameter measurements comparing manual and automatic segmentation methods (± two Standard Deviations (SD)).

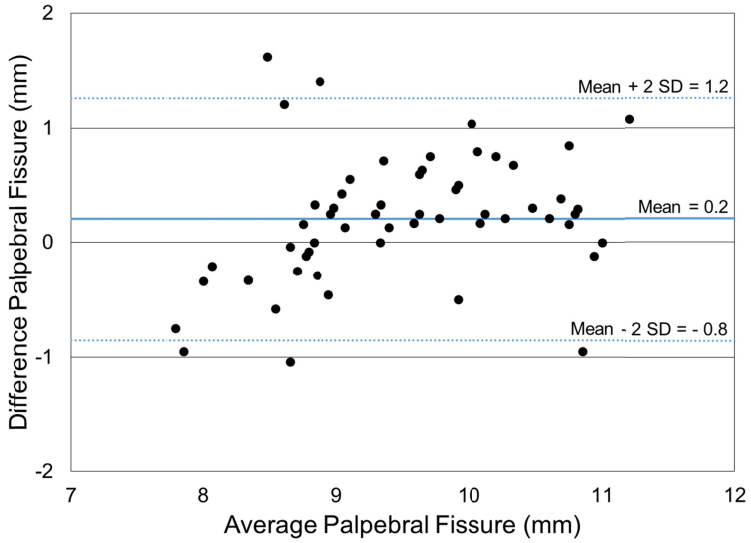

Fig. 11. Bland-Altman scatterplot of palpebral fissure height measurements comparing manual and automatic segmentation methods (± two Standard Deviations (SD)).

The pupil diameter (mm) and palpebral fissure height (mm) of the six healthy subjects used in the above analysis, as well as six achromatopsia subjects (4 females and 2 males, age = 14.3 ± 6.7 y/o, range: 6 to 23 y/o) was assessed and plotted versus VPT (log lux) (Fig. 12 and Fig. 13). The healthy subjects had a higher VPT, smaller baseline pupil diameter, higher percent change in pupil diameter, larger palpebral fissure height, and a lower percent change in palpebral fissure height when compared to the achromatopsia subjects. The healthy subject (ID#8) with the lowest VPT had a percent change in pupil diameter (24%) similar to the achromatopsia group. Overall, these results suggest that lower VPT may be associated with larger baseline pupil diameter, lower percent change in pupil diameter, smaller palpebral fissure height, and higher percent change in palpebral fissure height.

Biomedical Optics EXPRESS

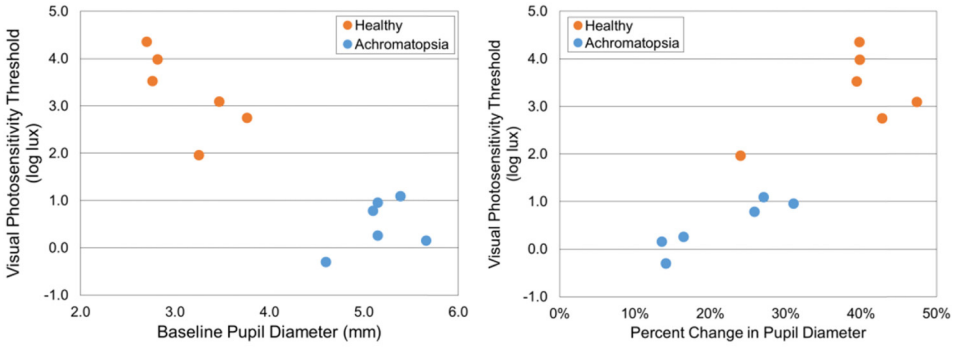

Fig. 12. Baseline pupil diameter (mm) and percent change in pupil diameter of six healthy and six achromatopsia subjects with respect to VPT (log lux).

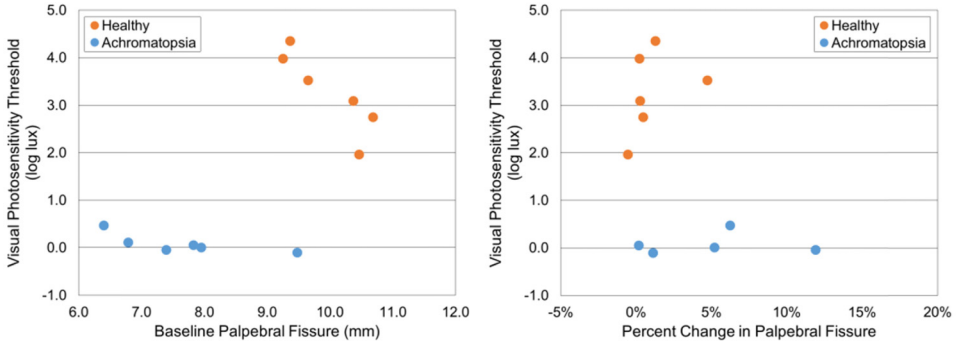

Fig. 13. Baseline palpebral fissure height (mm) and percent change in palpebral fissure height of six healthy and six achromatopsia subjects with respect to VPT (log lux).

5. Discussion

To the best of our knowledge, the OPA is the first instrument designed to provide a reliable and quantifiable measure of VPT in a clinical setting. The device will facilitate quantitative assessment of the efficacy of treatments for conditions associated with visual photosensitivity. The instrument design focused on reproducibility and scalability to enable longitudinal and multicenter studies. In addition to VPT, the system provides pupil diameter, palpebral fissure height, and inter-blink interval. These physiologic parameters will help provide a better understanding of the factors associated with visual photosensitivity. The performance of the OPA was evaluated in healthy and light sensitive (achromatopsia or traumatic brain injury) subjects. Light sensitive subjects manifested significantly lower VPT compared to healthy subjects. A longitudinal study revealed that the OPA reliably measured VPT in healthy subjects over one year. Another potential application of the OPA is to quantify light perception thresholds in subjects with vision in the bare light perception range.

The OPA presented in this study differs from the systems used in previous studies in that the determination of VPT is entirely automated and under subject's control. The synthesized speech provides instructions that reduce undesired operator bias and vocal cues, hence producing a more reliable measure. Also, unlike the halogen based system previously described [8,12,30,31] which provided a stimulus starting at an illuminance of 50.0 lux, the OPA can produce a stimulus starting at 1.5 lux allowing for more sensitive VPT measurements. Furthermore, by utilizing LEDs, the OPA produces a more stable output when compared to the halogen light source used in previous studies (Fig. 2) [8,12,30–32]. Lowering the voltage on tungsten halogen lamp produces changes in the spectra. The increased reliability and light output stability of the LEDs may enable more accurate testing in

Biomedical Optics EXPRESS

longitudinal studies. The spectral stability is especially important because visual photosensitivity is dependent on the light spectral input [42]. Further research is needed to investigate the relationship between light source spectrum and visual photosensitivity. Additionally, the effect of other parameters including age-related changes in spectral transmission of the crystalline lens as well as lens status (presence of cataract or intraocular lens), may impact the OPA VPT measurements and remain to be studied [43].

The ability to measure pupil diameter, palpebral fissure height and inter-blink interval will help provide deeper insight into the factors that contribute to visual photosensitivity and its variations across individuals or pathologies. For instance, our preliminary studies suggest that subjects with achromatopsia have a larger baseline pupil diameter than healthy subjects. On the other hand, the relative change in pupil diameter increases with the VPT in a manner that seems to be consistent in healthy and achromatopsia subjects. Eventually, we hope that the pupil diameter measurement will also enable predictions of the retinal irradiance at the VPT. Expressing the VPT in terms of retinal irradiance instead of illuminance may help eliminate confounding factors, such as the effects of variations in the pupil response. Furthermore, the relative change in palpebral fissure height remains mostly constant in healthy subjects whereas the achromatopsia subjects showed an increase in range.

One limitation of the present study is that refractive error was not taken into account in the analysis. All subjects wearing spectacles were tested without correction. Since each individual LED of the array forms its own separate small image on the retina, blur due to defocus could significantly reduce retinal irradiance. Therefore, uncorrected refractive error could be one of the factors that contributed to the inter-individual variability in VPT observed in our study. In principle, the measurements can be performed with untinted non-polarizing spectacles or contact lens correction.

Future studies with a larger sample size are warranted to determine the visual photosensitivity threshold differences between healthy subjects and subjects with conditions that affect light sensitivity such as dry eye, blepharospasm, migraine, traumatic brain injury, and retinal genetic disorders (achromatopsia and retinitis pigmentosa) and other retinal dysfunctions. Quantifying the visual photosensitivity thresholds of these individuals may help differentiate these different pathologies. Assessment tools for diagnosing visual photosensitivity have been limited [5]. Improving diagnostic measures and earlier detection criteria has the potential to improve treatment options especially assessing the effectiveness of novel gene therapies. The connection between visual photosensitivity and these pathologies is not clearly understood [19], in part because previous studies have reported visual changes in subjective terms which vary between fields and are not standardized. The OPA provides a reproducible and scalable method of measurement that will allow for a standardized measure of visual photosensitivity across studies.

Funding

National Eye Institute (NEI) (R24 EY022023, P30EY14801); Florida Lions Eye Bank and Beauty of Sight Foundation; Drs. KR Olsen and ME Hildebrandt; Drs. Raksha Urs and Aaron Hurtado; Society for Neuroscience – Neuroscience Scholars Program Associate (MCA); Brien Holden Vision Institute; an unrestricted grant from Research to Prevent Blindness; and the Henri and Flore Lesieur Foundation (JMP).

Acknowledgements

The authors acknowledge Anat Galor, MD and Potyra R. Rosa, MD of the Bascom Palmer Eye Institute, University of Miami Miller School of Medicine, Miami, FL for assistance with the recruitment of participants for this investigation. The authors thank David H. Sliney, Ph.D. and Andres Bernal, MS for their scientific contributions as well as the members of the Ophthalmic Biophysics Center team: Juan Silgado, BS; Kelly Mote, BS; Nidhi Relhan Batra, MD; Alejandro Arboleda, MS; William Lee; Nelson Salas, Ph.D.; Marco Ruggeri, Ph.D.;

Biomedical Optics EXPRESS

Varona Sargent, BS; Florence Cabot, MD; Mukesh Taneja, MD; Nicholas Nolan, BS; and Jeffrey Peterson, BS for their technical contributions. The authors would also like to thank Chelsea Skelley, Ph.D. and Joanna Johnson, Ph.D. of the University of Miami Writing Center for assistance in the preparation of this manuscript.

Disclosures

The authors declare that there are no conflicts of interest related to this article.

References

1. J. E. Lebensohn and J. Bellows, "The nature of photophobia," Arch. Ophthalmol. **12**(3), 380–390 (1934).
2. M. A. Mainster and P. L. Turner, "Glare's causes, consequences, and clinical challenges after a century of ophthalmic study," Am. J. Ophthalmol. **153**(4), 587–593 (2012).
3. B. J. Katz and K. B. Digre, "Diagnosis, pathophysiology, and treatment of photophobia," Surv. Ophthalmol. **61**(4), 466–477 (2016).
4. K. B. Digre and K. C. Brennan, "Shedding light on photophobia," J. Neuroophthalmol. **32**(1), 68–81 (2012).
5. Y. Wu and M. Hallett, "Photophobia in neurologic disorders," Transl. Neurodegener. **6**(1), 26 (2017).
6. A. Galor, R. C. Levitt, E. R. Felix, and C. D. Sarantopoulos, "What can photophobia tell us about dry eye?" Expert Rev. Ophthalmol. **11**(5), 321–324 (2016).
7. P. Rosenthal and D. Borsook, "Ocular neuropathic pain," Br. J. Ophthalmol. **100**(1), 128–134 (2016).
8. W. H. Adams, K. B. Digre, B. C. Patel, R. L. Anderson, J. E. Warner, and B. J. Katz, "The evaluation of light sensitivity in benign essential blepharospasm," Am. J. Ophthalmol. **142**(1), 82–87 (2006).
9. K. B. Digre, "Benign essential blepharospasm–there is more to it than just blinking," J. Neuroophthalmol. **35**(4), 379–381 (2015).
10. M. K. Blackburn, R. D. Lamb, K. B. Digre, A. G. Smith, J. E. A. Warner, R. W. McClane, S. D. Nandedkar, W. J. Langeberg, R. Holubkov, and B. J. Katz, "FL-41 tint improves blink frequency, light sensitivity, and functional limitations in patients with benign essential blepharospasm," Ophthalmology **116**(5), 997–1001 (2009).
11. H. L. Rossi and A. Recober, "Photophobia in primary headaches," Headache **55**(4), 600–604 (2015).
12. J. Vanagaite, J. A. Pareja, O. Støren, L. R. White, T. Sand, and L. J. Stovner, "Light-induced discomfort and pain in migraine," Cephalalgia **17**(7), 733–741 (1997).
13. S. M. Llop, J. E. Frandsen, K. B. Digre, B. J. Katz, A. V. Crum, C. Zhang, and J. E. A. Warner, "Increased prevalence of depression and anxiety in patients with migraine and interictal photophobia," J. Headache Pain **17**(1), 34 (2016).
14. A. Main, A. Dowson, and M. Gross, "Photophobia and phonophobia in migraineurs between attacks," Headache **37**(8), 492–495 (1997).
15. A. Main, I. Vlachonikolis, and A. Dowson, "The wavelength of light causing photophobia in migraine and tension-type headache between attacks," Headache **40**(3), 194–199 (2000).
16. E. P. Chronicle and W. M. Mulleners, "Visual system dysfunction in migraine: a review of clinical and psychophysical findings," Cephalalgia **16**(8), 525–535 (1996).
17. R. Noseda, D. Copenhagen, and R. Burstein, "Current understanding of photophobia, visual networks and headaches," Cephalalgia **0**(0), 333102418784750 (2018).
18. K. B. Digre, "More Than Meets the Eye: The Eye and Migraine-What You Need to Know," J. Neuroophthalmol. **38**(2), 237–243 (2018).
19. P. T. Yuhas, P. D. Shorter, C. E. McDaniel, M. J. Earley, and A. T. Hartwick, "Blue and red light-evoked pupil responses in photophobic subjects with TBI," Optom. Vis. Sci. **94**(1), 108–117 (2017).
20. B. P. Barnett and E. L. Singman, "Vision concerns after mild traumatic brain injury," Curr. Treat. Options Neurol. **17**(2), 329 (2015).
21. C. S. Gilmore, J. Camchong, N. D. Davenport, N. W. Nelson, R. H. Kardon, K. O. Lim, and S. R. Sponheim, "Deficits in visual system functional connectivity after blast-related mild TBI are associated with injury severity and executive dysfunction," Brain Behav. **6**(5), e00454 (2016).
22. F. Barker, G. Cockerham, G. Goodrich, A. Hartwick, R. Kardon, A. B. Mick, and M. Swanson, "Brain injury impact on the eye and vision," Optom. Vis. Sci. **94**(1), 4–6 (2017).
23. H. Laukkanen, M. Scheiman, and J. R. Hayes, "Brain injury vision symptom survey (BIVSS) questionnaire," Optom. Vis. Sci. **94**(1), 43–50 (2017).
24. D. Stern, "Photophobia, light, and color in acquired brain injury," in *Vision Rehabilitation* (CRC Press, 2011), pp. 283–300.
25. M. L. Callahan and M. M. Lim, "Sensory Sensitivity in TBI: Implications for Chronic Disability," Curr. Neurol. Neurosci. Rep. **18**(9), 56 (2018).
26. J. Aboshiha, A. M. Dubis, J. Carroll, A. J. Hardcastle, and M. Michaelides, "The cone dysfunction syndromes," Br. J. Ophthalmol. **100**(1), 115–121 (2016).
27. J. D. Wirtschafter, C. M. Bourassa, and R. S. Dow, "The Quantitative Study of Photophobia," Trans. Am. Neurol. Assoc. **88**, 291–293 (1963).

Biomedical Optics EXPRESS

28. J. D. Wirtschafter and C. M. Bourassa, "Binocular Facilitation of Discomfort with High Luminances," Arch. Ophthalmol. **75**(5), 683–688 (1966).
29. C. M. Bourassa and J. D. Wirtschafter, "Mechanism of binocular increase of discomfort to high luminance," Nature **212**(5069), 1503–1504 (1966).
30. J. Vanagaite Vingen and L. J. Stovner, "Photophobia and phonophobia in tension-type and cervicogenic headache," Cephalalgia **18**(6), 313–318 (1998).
31. J. V. Vingen, J. A. Pareja, and L. J. Stovner, "Quantitative evaluation of photophobia and phonophobia in cluster headache," Cephalalgia **18**(5), 250–256 (1998).
32. M. M. Cortez, N. A. Rea, L. A. Hunter, K. B. Digre, and K. C. Brennan, "Altered pupillary light response scales with disease severity in migrainous photophobia," Cephalalgia **37**(8), 801–811 (2017).
33. C. Hood and M. A. Finkelstein, "Sensitivity to light" in *Handbook of Perception and Human Performance* - Vol. 1: Sensory Processes and Perception (John Wiley & Sons, Inc., 1986), pp. 1–66.
34. J. C. Stevens and S. S. Stevens, "Brightness function: effects of adaptation," J. Opt. Soc. Am. **53**(3), 375–385 (1963).
35. M. A. García-Pérez, "Yes-no staircases with fixed step sizes: psychometric properties and optimal setup," Optom. Vis. Sci. **78**(1), 56–64 (2001).
36. M. A. García-Pérez, "Adaptive psychophysical methods for nonmonotonic psychometric functions," Atten. Percept. Psychophys. **76**(2), 621–641 (2014).
37. B. Golebiowski, E. Papas, and F. Stapleton, "Corneal mechanical sensitivity measurement using a staircase technique," Ophthalmic Physiol. Opt. **25**(3), 246–253 (2005).
38. A. J. Zele and D. Cao, "Vision under mesopic and scotopic illumination," Front. Psychol. **5**(1594), 1594 (2015).
39. J. L. Fleiss, "Reliability of Measurement," in *The Design and Analysis of Clinical Experiments* (John Wiley & Sons, Inc., 1999), pp. 1–32.
40. D. G. Altman and J. M. Bland, "Measurement in Medicine: The Analysis of Method Comparison Studies," Statistician **32**(3), 307–317 (1983).
41. J. M. Bland and D. G. Altman, "Measuring agreement in method comparison studies," Stat. Methods Med. Res. **8**(2), 135–160 (1999).
42. J. M. Stringham, K. Fuld, and A. J. Wenzel, "Action spectrum for photophobia," J. Opt. Soc. Am. A **20**(10), 1852–1858 (2003).
43. Y. Sakanishi, M. Awano, A. Mizota, M. Tanaka, A. Murakami, and K. Ohnuma, "Age-related changes in spectral transmittance of the human crystalline lens in situ," Ophthalmologica **228**(3), 174–180 (2012).